Asian Journal of Applied Sciences (ISSN: 2321 – 0893)
Volume 02 – Issue 04, August 2014

Periodic Laminar Forced Convection in a Circular Tube with Double Twisted Tapes

Amnart Boonloi

Department of Mechanical Engineering Technology, College of Industrial Technology,
King Mongkut's University of Technology North Bangkok, Bangkok 10800, Thailand.
Email: amnartb {at} kmutnb.ac.th

ABSTRACT—*Fully developed laminar flow and heat transfer behavior in a circular tube with double twisted tapes are presented numerically. The computational domain is solved by the finite volume method. The numerical results are presented for Reynolds number, Re = 100 – 2000. The influences of the double twisted tapes; twisted ratio (y/W, TR = 1–6) and rotations of the twisted tapes (co–rotating and counter–rotating), on heat transfer, flow structure and thermal performance are studied and compared with single twisted tape under similar conditions. The use of the double twisted tapes can create swirl flows over the test section that helps to improve heat transfer rate and thermal performance. The rise of TR leads to decrease in Nusselt number and friction factor values. The co–rotating twisted tapes case gives higher level of vortex strength and thermal performance than the counter–rotating twisted tapes case, but provides nearly value of friction factor. In range studies, the optimum thermal enhancement factors, TEF are around 2.70 and 2.30 for the co–rotating and counter–rotating cases, respectively.*

Keywords— circular tube, double twisted tapes, laminar flow, heat transfer, pressure loss, periodic flow

---

1. INTRODUCTION

Rising-worldwide energy demand and increasing consumption have been resulted in an increased effort to create high performance heat exchanger equipment. Various techniques for enhancing heat transfer are widely applied in heating systems in order to augment heat transfer and thermal performance. The twisted tape vortex generators had been widely adopted for improving thermal performance in the heat exchanger channel. The appearances of the boundary layer, inducing flow and swirling flow are appearing when installed with twisted tape that help to enhance the heat transfer rate. Except for the heat transfer augmentation and thermal performance improvement, it is found that the presence of the twisted tape leads to the rise of the pressure loss in the system. Therefore, the main aim to design of the twisted tape must be considered on both the heat transfer rate and pressure loss.

The experimental investigations for heat transfer improvement by using twisted tapes have been extensively reported. Eiamsa–ard et al. [1] experimental studied the effect of short–length and full length twisted tapes in a circular tube on heat transfer, friction factor and thermal performance. They reported that the short length twisted tapes perform lower heat transfer, friction factor as well as enhancement efficiency than the full length tape insert. Eiamsa–ard et al. [2] investigated the regularly spaced twisted tape in double pipe heat exchanger on heat transfer behavior and flow configurations. They claimed that the increases in heat transfer and friction factor are found when reducing twisted ratio. Pal and Saha [3] experimental studied the combined generators; spiral–corrugate–tube and twisted tape with oblique teeth for the laminar flow regime. They summarized that the combined generators provide higher thermal performance than the single generators. Pal and Saha [4] also studied combination of the vortex generators between transverse–corrugate–tube and center–cleared twisted–tape on heat transfer and friction loss by experimental method. Chang and Guo [5] investigated the thermal performance enhancement in heat exchanger with continuous and spiky twisted tapes. They reported that the V–notched spiky twisted tape gives the highest on both heat transfer rate and thermal performance. Promvonge et al. [6] studied the heat transfer augmentation in a helical–ribbed tube with double twisted tapes. They concluded that the *TR* = 8 performs the highest on thermal performance at lower *Re* values. Bas and Ozceyhan [7] presented the effects of twisted ratios and clearance ratios for twisted tape in the test tube at turbulent regime. They found that the optimum thermal performance is around 1.756 at clearance ratio of 0.0178, *TR* = 2 and *Re* = 5183. Bhuiya et al. [8] studied the influences of double counter twisted tapes for a turbulent regime with experimental method. They found that the decrease of the twisted ratio results in the rise of heat transfer, thermal performance and friction loss. They also showed that the augmentations are around 60 – 240% and 91 – 286% for heat transfer and friction loss, respectively, in comparison to the smooth tube. Eiamsa–ard et al.[9] experimental investigated on heat transfer, friction loss and thermal performance in circular tube with helically twisted tapes. They reported that the highest thermal performance is around 1.29 at *TR* = 3. Bhuiya et al. [10] presented the effects of triple twisted tapes on thermal performance for turbulent force convection with experimental technique. They found that the enhancements are around 3.85 and 4.2 times higher than the smooth channel with no generators and thermal performance is found to be about 1.44 at similar pumping power. Bhuiya et al. [11] reported that the enhancements of the heat transfer, pressure loss and thermal performance are found to be around 110–340%, 110–360% and 28–59%, respectively, for the perforated twisted tape when compared with smooth case. Chang et al. [12] investigated the influence of the twisted ratio for broken–twisted tapes in a tube on heat transfer and friction loss. They concluded that the reduction of the twisted ratio leads to the increase on both heat transfer rate and pressure loss of the heating system. Seemawute [13] presented uniform heat flux circular tube inserted with peripherally–cut twisted tape with alternate axis on heat transfer improvement. Bhattacharyya and Saha [14] presented that the combined turbulators (center–cleared twisted tapes and helical rib) provide higher thermal performance than the single turbulators. Thianpong et al. [15] studied the combined turbulators (perforated twisted tapes and parallel wings) on heat transfer improvement in heat exchanger tube. They pointed out that the combined turbulators give higher heat transfer rate around 208% when compared with the plain tube. Promvonge and Eiamsa–ard [16] reported the influences of the combined turbulators; conical–ring and twisted tape in circular tube on thermal performance. They summarized that the combined turbulators perform better thermal performance than the use of the conical–ring only. Eiamsa–ard et al. [17] investigated the heat transfer behavior, flow characteristic and thermal performance in heat exchanger with regularly–spaced twisted tape on both numerical and experimental methods. They claimed that the numerical method can help to describe the flow structure and heat transfer configuration in the test channel. They also concluded that the decreases in twisted ratio and space ratio lead to the rise of the heat transfer and pressure loss. Eiamsa–ard et al. [18] numerically investigated the swirling flow in a tube by loose–fit twisted tape insertion. Zhang et al. [19] numerical investigated on heat transfer behavior in a tube with triple and quadruple twisted tapes. They presented that the optimum heat transfer enhancements are around 171% and 182%, respectively, for triple and quadruple twisted tapes. Guo et al. [20] numerically studied the effect of center–cleared twisted tape in circular tube on both heat transfer and friction factor characteristics for the laminar flow regime. They showed that the center–cleared twisted tape placed in the tube can enhance heat transfer around 7–20% when compared with the conventional twisted tape. Eiamsa–ard and Seemawute [21] examined the effects of short–length twisted tapes in heat exchanger tube on thermal performance. They found that the short–length twisted tapes can help to reduce pressure loss in the heating system. Hong et al. [22] numerical investigated the influences of twin twisted tapes in the tube at turbulent regime. They summarized that the use of the twin twisted tapes, performs higher heat transfer rate than the base case around 6.3 – 35.7%.

Except from experimental and numerical investigation above, the study on mechanism of heat transfer enhancement that could serve as a guideline to optimize compact heat exchangers and design new type heat transfer enhancement apparatus are presented as Ref. [23–26].

Jedsadaratanachai and Boonloi [27] presented the effect of twisted ratio, *TR* = 1 – 6, for single twisted tape in a circular tube at laminar regimes, *Re* = 100 – 2000. They found that the single twisted tape performs higher thermal enhancement factor than the smooth tube, especially, at *TR* = 6, due to low friction factor value.

According to Ref. [27], it is noticed that the *TR* = 6 of the single twisted tape provides the highest of TEF, but produces the lowest heat transfer rate. Therefore, the study of the modified–twisted tape which helps to increase on both heat transfer rate and thermal performance is presented. In this work, the numerical investigations on heat transfer, pressure loss and thermal performance in a circular tube with the double twisted tapes are presented and compared with previous research, the single twisted tape [27]. The double twisted tapes can create two main of swirl flows that lead to better heat transfer distributions over the tube wall. Due to the *TR* = 1 on both the single twisted tape and double twisted tapes show very enlarge pressure loss, therefore, this present research is focused on the effects of twisted ratio (*TR* = 2–6) and tape rotation (co–rotating, counter–rotating) for Reynolds number, *Re* = 100–2000.

2. PHYSICAL MODELS AND NUMERICAL METHOD

2.1 Physical models

The double twisted tapes which insert in a circular tube with co–rotating and counter–rotating are presented as Figs. 1a and b, respectively. The details of the double twisted tapes are displayed in Fig. 1c. The fully developed periodic flow and heat transfer conditions apply for the computational domain. The concepts of periodical fully stabilized flow and its solution procedure are described in Ref. [23 – 27]. Air enters the circular tube at an inlet temperature, T_{in}, and flows though the test section. The width for each of twisted tape, W, twisted pitch length, y, and y/W is known as twisted ratio, *TR*. The tube diameter, D and the diameter ratio, W/D are fixed as 0.5 for all cases. All case studies are presented in Table 1.

Table 1: Double twisted tape cases.

Case	*Rotation*	y/W	W/D	*Re*
I	co–rotating	2 – 6	0.5	100 – 2000
II	counter–rotating	2 – 6	0.5	100 – 2000

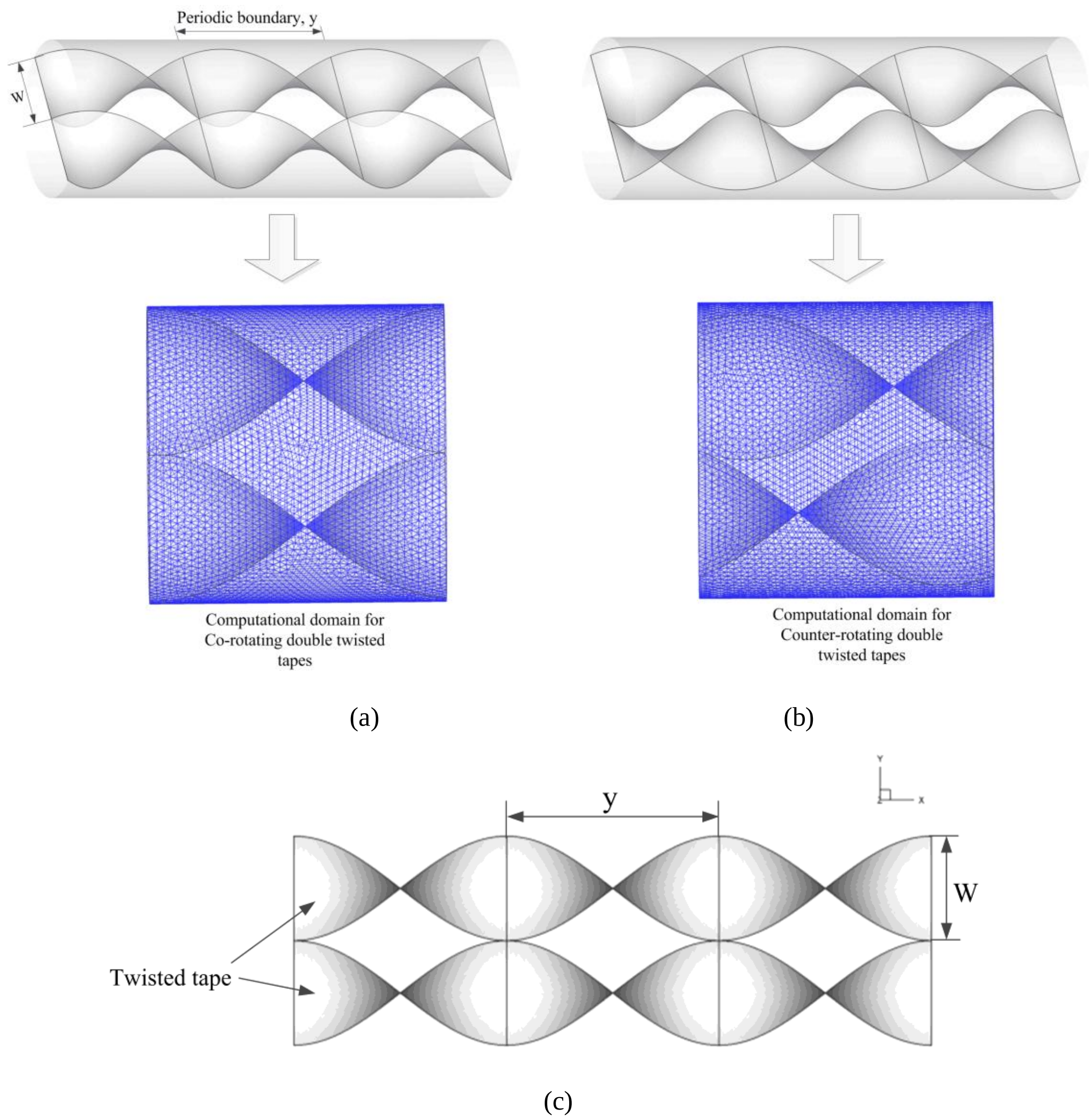

Figure 1: (a) tube geometry and computational domain for co–rotating case and (b) tube geometry and computational domain for counter–rotating case and (c) details of double twisted tapes.

2.2 Boundary conditions

According to Refs. [23 – 27], the circular tube wall is set at the constant temperature at 310 K while the double twisted tapes are assumed at adiabatic wall condition. The inlet and outlet of the domain are set as identically velocity profiles. The air temperature is set as 300 K (Pr = 0.7) at the inlet of the domain and enters to test tube with constant mass flow rate. The constant condition of the air properties at average bulk temperature is used. The tube wall and twisted tape surfaces are set as impermeable boundary and no–slip wall conditions.

2.3 Numerical models

The assumptions of the computational model for flow and heat transfer are as follows:

- The fluid flow and heat transfer are assumed to be steady state in three–dimensional.
- The tested flow is fixed in laminar regime and incompressible.
- The fluid properties remain constant.
- The Body forces, viscous dissipation and radiation heat transfer are supposed to be neglected.

2.4 Grid system

The four differences number of grid cells; 120,000, 290,000, 350,000 and 430,000 cells are used to test the grid convergence index. As results, the variations on both *Nu* and *f* for the double twisted tapes at *TR* = 2 and *Re* = 1000 is less than 0.2% when increasing grid cell from 290,000 to 350,000. Therefore, the grid of 290,000 cells applies for current computational domain considering on both convergent time and solution precision.

3. MATHEMATICAL FOUNDATIONS

Based on the above assumptions, equations of continuity, momentum and energy for the fluid flow are given below in a tensor form as Eqs. 1, 2 and 3, respectively.

Continuity equation:

$$\frac{\partial}{\partial x_i}(\rho u_i) = 0 \tag{1}$$

Momentum equation:

$$\frac{\partial(\rho u_i u_j)}{\partial x_j} = -\frac{\partial p}{\partial x_i} + \frac{\partial}{\partial x_j}\left[\mu\left(\frac{\partial u_i}{\partial x_j} + \frac{\partial u_j}{\partial x_i}\right)\right] \tag{2}$$

Energy equation:

$$\frac{\partial}{\partial x_i}(\rho u_i T) = \frac{\partial}{\partial x_j}\left(\Gamma \frac{\partial T}{\partial x_j}\right) \tag{3}$$

where Γ is the thermal diffusivity and is given by

$$\Gamma = \frac{\mu}{Pr} \tag{4}$$

The governing equations are discretized by the second order upwind (SOU) scheme while the energy equation is discretized by the QUICK scheme. The SIMPLE algorithm and finite volume method [28] are used in the present computational domain. The solutions are considered to be converged when the normalized residual values were less than 10^{-5} for all variables, but less than 10^{-9} only for the energy equation.

The Reynolds number, friction factor, Nusselt number and thermal enhancement factor are calculated as follows:

$$Re = \rho UD/\mu \tag{5}$$

The friction factor, *f*, is computed by pressure drop, Δp, across the length of the periodic tube, *L*, as

$$f = \frac{2(\Delta p/L)D}{\rho U^2} \tag{6}$$

The heat transfer is measured by the local Nusselt number which can be written as

$$Nu = \frac{hD}{k} \tag{7}$$

The average Nusselt number can be obtained by

$$Nu = \frac{1}{A}\int Nu_x \partial A \tag{8}$$

According to Ref. [27], the thermal enhancement factor (*TEF*) is defined as the ratio of the heat transfer coefficient of an augmented surface, *h* to that of a smooth surface, h_0, at an equal pumping power and given by

$$TEF = \left.\frac{h}{h_0}\right|_{pp} = \left.\frac{Nu}{Nu_0}\right|_{pp} = (Nu/Nu_0)/(f/f_0)^{1/3} \tag{9}$$

where Nu_0 and f_0 stand for Nusselt number and friction factor for the smooth tube, respectively.

4. RESULTS AND DISCUSSION

4.1 Validation of smooth circular tube

Table 2 shows the verifications of heat transfer and pressure loss for smooth circular tube with no twisted tapes by comparison between the values from exact solution and present prediction. The heat transfer and friction factor are presented in terms of Nusselt number and friction factor, respectively.

Table 2: Validations of smooth tube.

Re	***Exact solution***		***Present prediction***		***Error (%)***	
	Nu	***f***	***Nu***	***f***	***Nu***	***f***
100	3.6600	0.6400	3.6560	0.6415	-0.1093	0.2344
200	3.6600	0.3200	3.6640	0.3199	0.1093	-0.0312
300	3.6600	0.2133	3.6640	0.2131	0.1093	-0.0938
400	3.6600	0.1600	3.6640	0.1601	0.1093	0.0625
500	3.6600	0.1280	3.6640	0.1281	0.1093	0.0781
600	3.6600	0.1067	3.6640	0.1068	0.1093	0.0937
800	3.6600	0.0800	3.6640	0.0802	0.1093	0.2500
1000	3.6600	0.0640	3.6640	0.0641	0.1093	0.1563
1200	3.6600	0.0533	3.6640	0.0531	0.1093	-0.3752
1600	3.6600	0.0400	3.6640	0.0400	0.1093	0.0000
2000	3.6600	0.0320	3.6640	0.0320	0.1093	0.0000

The results show agrees well within ±0.40% on both Nusselt number and friction factor. Therefore, the present numerical domain has reasonable accuracy. The exact solution of the Nusselt number is displayed as Eq. 10 while Eq. 11 presents the exact solution of the friction factor for laminar flows over smooth tube with constant wall temperature [29]:

$$Nu_0 = 3.66 \tag{10}$$

$$f_0 = 64/Re \tag{11}$$

4.2 Flow configuration

The flow configurations for laminar flow over the double twisted tapes in the circular tube are shown in terms of streamlines in transverse planes and streamlines in three dimensional or swirl flow though the test section as Figs. 2 – 5.

Figs. 2a and b present the streamlines in transverse planes for co–rotating case and counter–rotating case of the double twisted tapes, respectively, at *TR* = 2 and *Re* = 800. In general, the co–rotating case performs four main vortex flows while the counter–rotating case provides two main of vortex flows. Co–rotating case, the two differences of the vortex types; vortex which created from the twisted tape directly and induced vortex, are found as depicted in Fig. 3a. Counter–rotating case, two main vortices with common–flow–down that introduced from double twisted tapes directly are found as displayed in Fig. 3b. Figs. 3c and d present the details of the streamlines in transverse planes for the double twisted tapes at co–rotating case and counter–rotating case, respectively. It is clearly seen that the core of the main vortex which created from the twisted tape directly has no change in the position while the core of the induced vortex flow in case of the co–rotating double twisted tapes has slightly different.

Figs. 4a and b present streamlines flow over the test tube in three dimensions for co–rotating case and counter–rotating case, respectively. It is found that the flows on both cases are swirling over surface of the double twisted tapes depended on the direction of the twist.

Figs. 5a, b, c and d illustrate the streamlines in transverse planes for co–rotating double twisted tapes at *Re* = 1000 for *TR* = 2, 3, 4, 5 and 6, respectively. In general, the flow structures of the double twisted tapes at various twisted ratios are seen similar; the doubles twisted tapes perform two main vortices which created directly from twisted tapes and two inducted vortices.

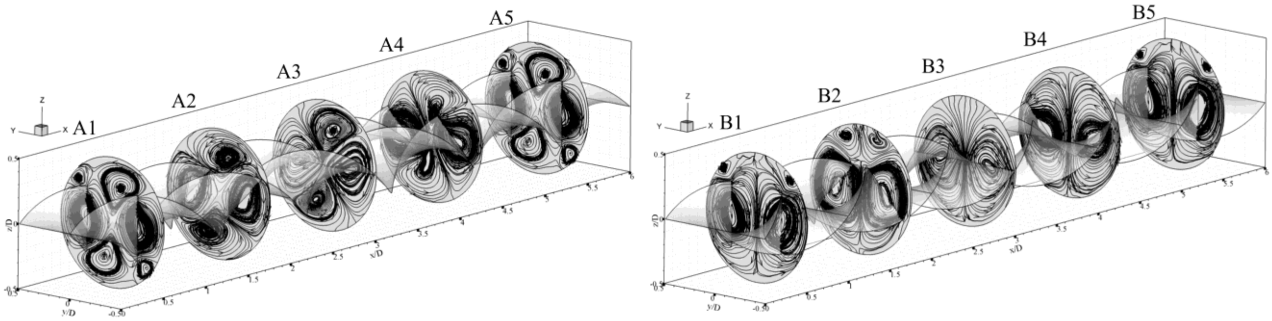

(a) (b)

Figure 2: Streamlines in transverse planes for (a) co–rotating case and (b) counter–rotating case of double twisted tapes at *Re* = 800 and *TR* = 2.

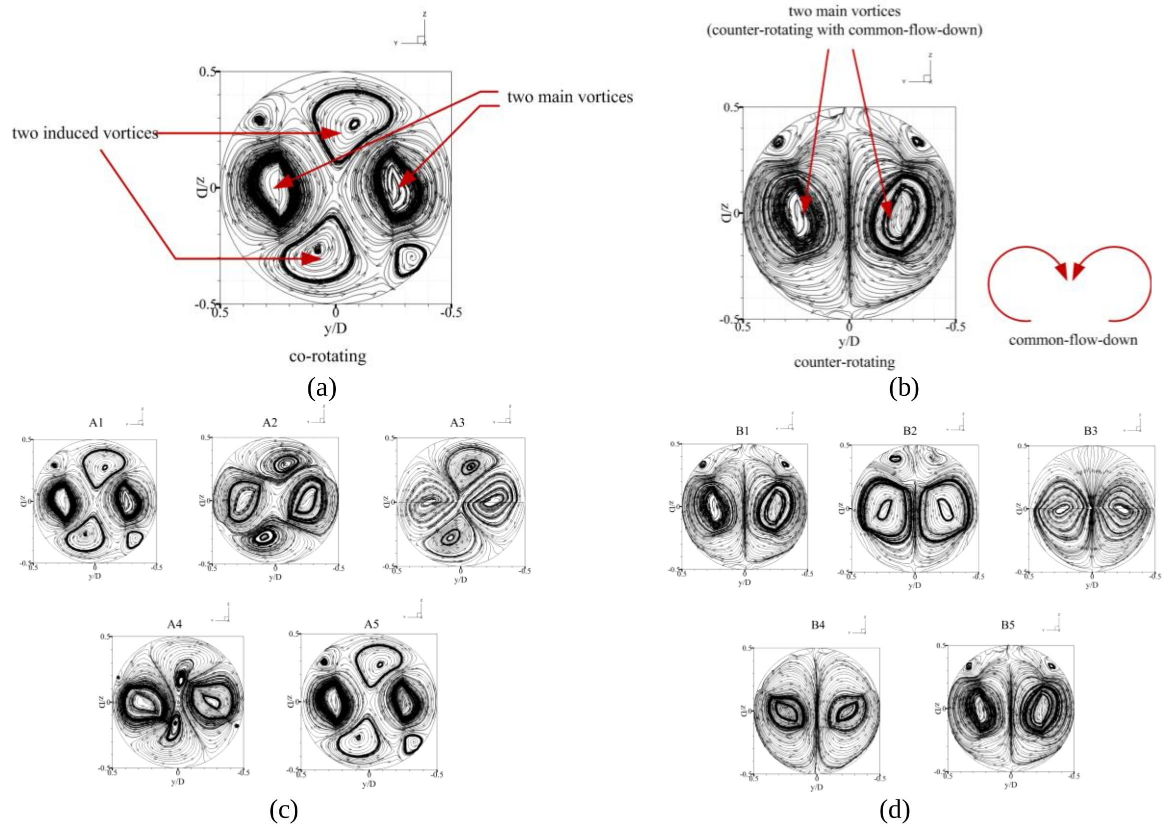

Figure 3: Details of Streamlines in transverse planes for (a) co–rotating case, (b) counter–rotating case, (b) co–rotating case planes A1–A5 and (d) counter–rotating case planes B1–B5 for double twisted tapes at *Re* = 800 and *TR* = 2.

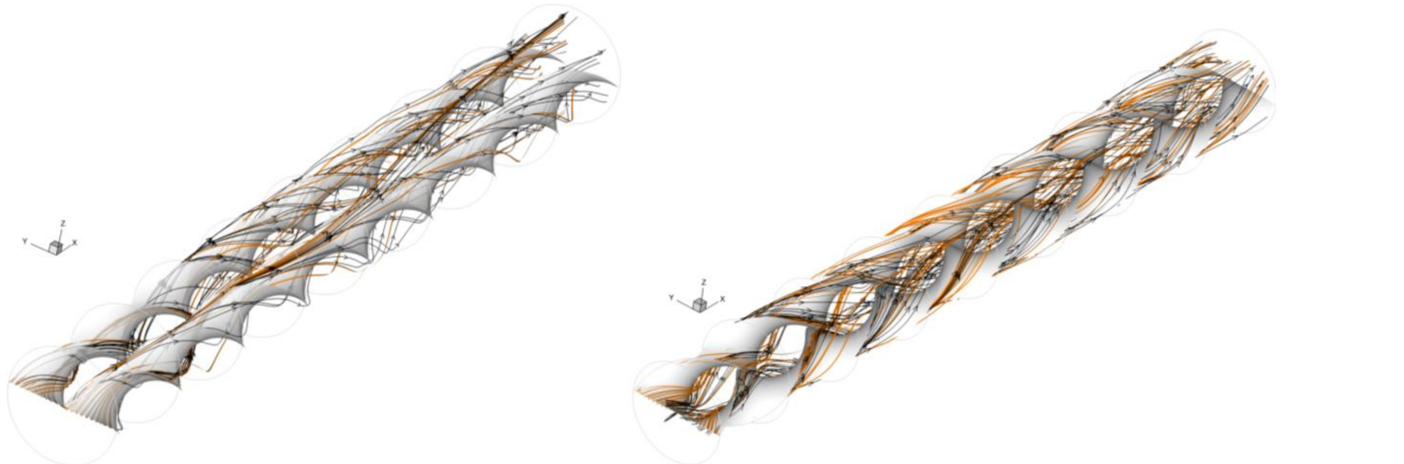

(a) (b)

Figure 4: 3D swirling flows over the double twisted tapes surface for (a) co–rotating case and (b) counter–rotating case of double twisted tapes at *Re* = 800 and *TR* = 2.

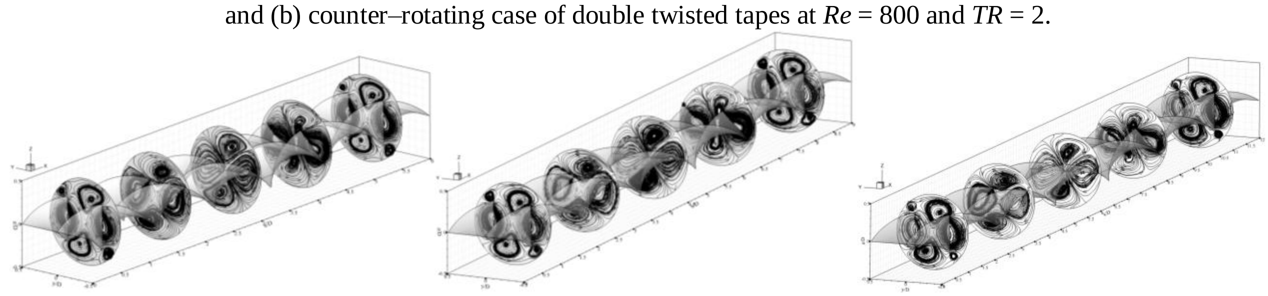

(a) (b) (c)

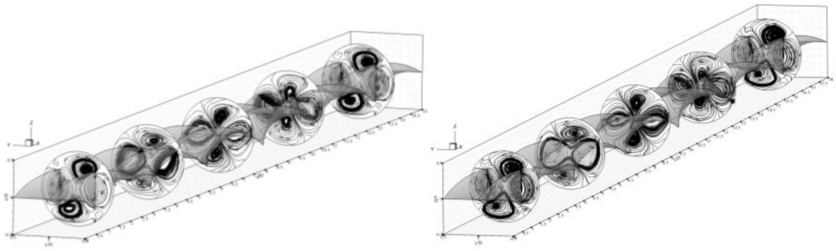

(d) (e)

Figure 5: Streamlines in transverse planes for co–rotating double twisted tapes (a) TR = 2, (b) TR = 3, (c) TR = 4, (d) TR = 5 and (e) TR = 6 at Re = 1000.

4.3 Heat transfer characteristic

The heat transfer characteristics for the double twisted tapes in the circular tube are presented in terms of temperature contours in transverse planes and local Nusselt number contours as Figs. 6 – 10.

Figs. 6a and b show contours of temperature in transverse planes for co–rotating case and counter–rotating case, respectively, while the details of temperature contours in transverse planes are displayed in Fig. 7. As the figures, the use of double twisted tapes provides good mixing of fluid flow in comparison with smooth circular tube. This means that the vortex flows or swirl flows are an important factor of the influence on the temperature field; it can induce better fluid mixing between near the wall and the core region, leading to high temperature gradient over the heating wall. In addition, the numerical results reveal that the co–rotating case provides better mixing of the tested fluid than the counter–rotating case when considering at the thermal boundary layer thickness. The heat transfer characteristics with various twisted ratios perform an identical prototype for all cases as depicted in Figs. 8.

Local Nu_x contours over the tube wall with the co–rotating and counter–rotating cases are shown in Figs. 9a and b, respectively. For co–rotating double twisted tapes, the tube wall near the two main vortices that created from the double twisted tapes shows the highest heat transfer rate while the area of tube wall near induced vortices give the lowest heat transfer rate. For counter–rotating case, the peak of Nu_x is found at the lower part of tube wall that according to the flow structure, counter–rotating with common–flow–down and impinging flow at the lower part of the test tube.

The local Nusselt number distributions over the tube wall with various TR values are presented as depicted in Figs. 10a to e for TR = 2, 3, 4, 5 and 6, respectively, for co–rotating cases. It is seen that the increase in twisted ratio leads to decrease in Nusselt number. Additional, TR = 6 provides the lowest values of the Nusselt number while TR = 1 performs the highest value.

Figs. 11a and b present the variations of Nu/Nu_0 with Reynolds number and TR, respectively, for double twisted tapes. In general, Nu/Nu_0 value tends to increase with the rise of Reynolds number, but decreases with increasing TR for all cases. The co–rotating case performs higher heat transfer rate than counter-rotating case when the Reynolds number higher than 800. The co–rotating case with TR = 2 provides the highest Nu/Nu_0 while TR = 6 of counter-rotating case shows the lowest values of Nu/Nu_0. In range studies, the use of double twisted tapes provides heat transfer rate higher than the smooth circular tube about 1.4 – 7.3.

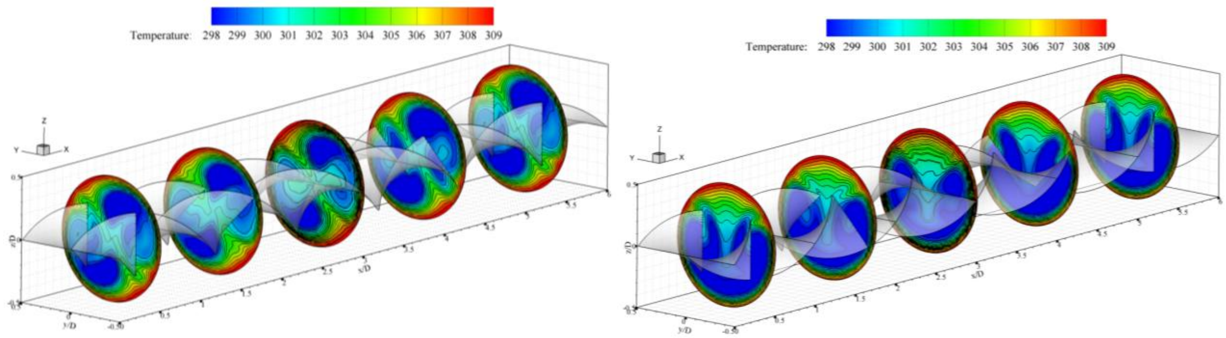

(a) (b)

Figure 6: Temperature contours in transverse planes for (a) co–rotating case and (b) counter–rotating case of double twisted tapes at Re = 800 and TR = 2.

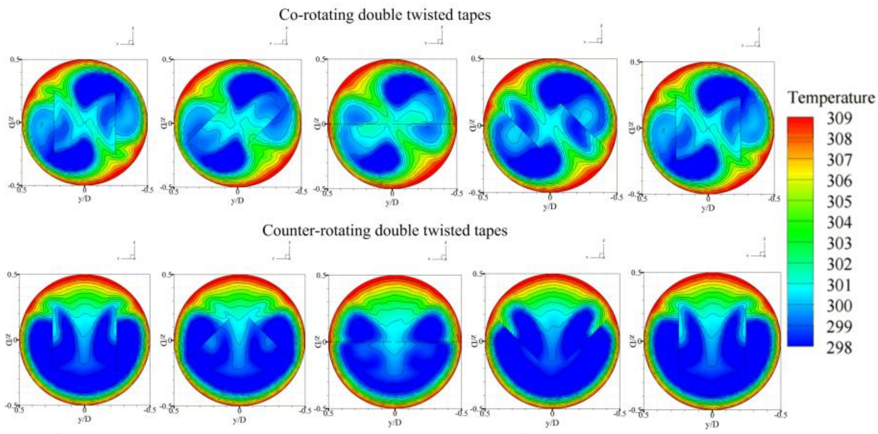

Figure 7: Details of temperature contours in transverse planes for double twisted tapes at *Re* = 800 and *TR*. = 2.

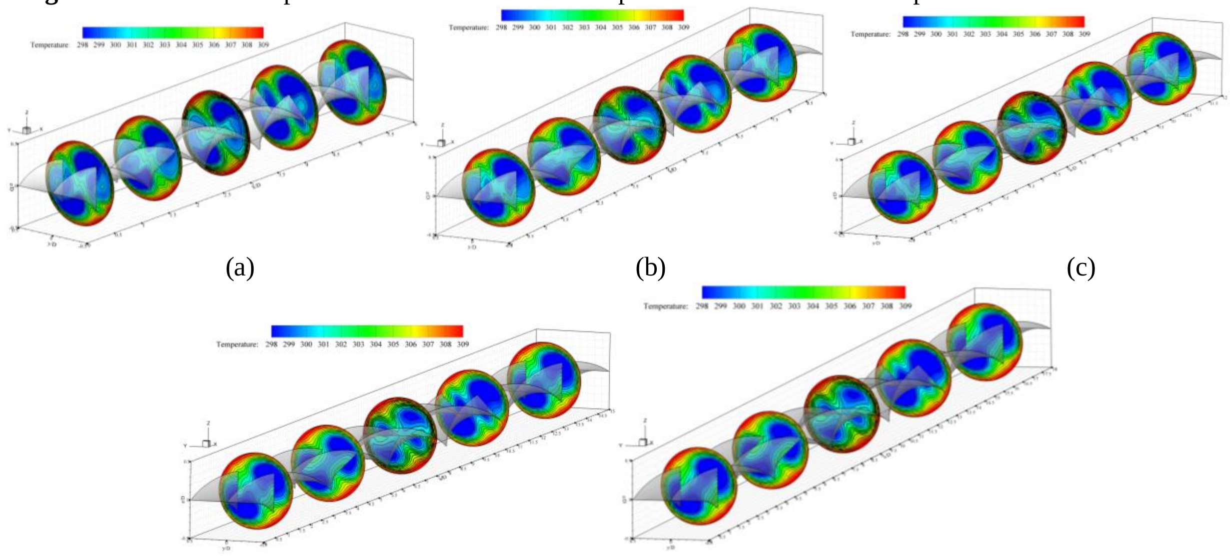

(a) (b) (c)

(d) (e)

Figure 8: Temperature contours in transverse planes for co–rotating double twisted tapes (a) *TR* = 2, (b) *TR* = 3, (c) *TR* = 4, (d) *TR* = 5 and (e) *TR* = 6 at *Re* = 1000.

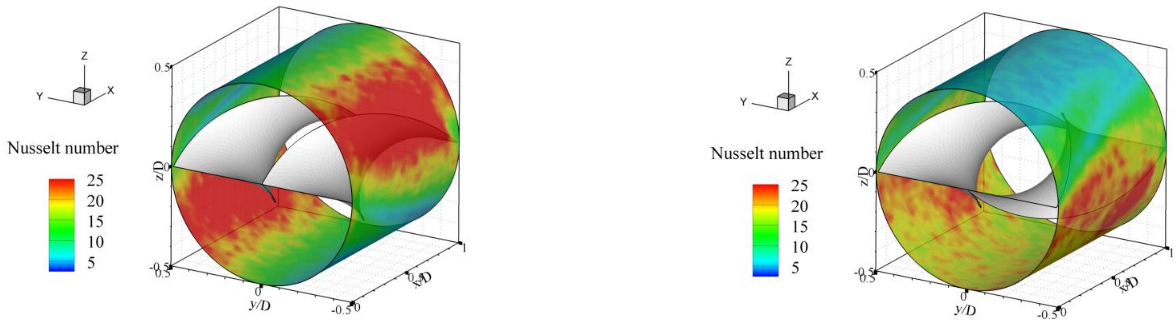

(a) (b)

Figure 9: Nu_x Contours for (a) co–rotating case and (b) counter–rotating case of double twisted tapes at *Re* = 800 and *TR* = 2.

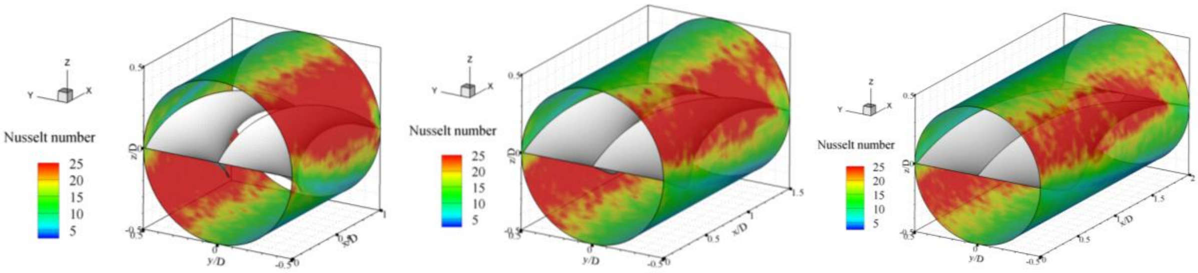

(a) (b) (c)

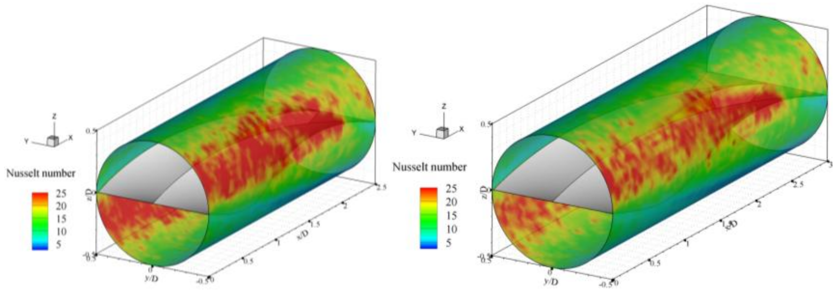

(d) (e)

Figure 10: Nu_x Contours for co–rotating double twisted tapes (a) *TR* = 2, (b) *TR* = 3, (c) *TR* = 4, (d) *TR* = 5 and (e) *TR* = 6 at *Re* = 1000.

4.4 Pressure loss

Figs. 12a and b present the variations of friction factor, f/f_0 with Reynolds number values and with *TR*, respectively, for double twisted tapes. The f/f_0 tends to increase with the rise of Reynolds number and reducing the *TR* value for all cases. Due to the similar twisted ratio of the double twisted tapes configuration in cross sectional area, the f/f_0 values on both cases show nearly values for the laminar flow regime. In the range of studies, the maximum f/f_0 is found to be about 18.5 for the co–rotating double twisted tapes with *TR* = 2 and Re = 2000. The f/f_0 varies in the range 3.5 – 18.5 depended on Reynolds number, twisted ratio and twisted rotation.

4.5 Performance evaluation

The variations of thermal enhancement factor (*TEF*) with Reynolds number are illustrated in Fig. 13a while the variations of the *TEF* with *TR* values are displayed as Fig. 13b. The enhancement factor of both cases tends to increase with the rise of Reynolds number, but slightly decrease with the increase of twisted ratio. In range studies, the use of double twisted tapes gives the thermal enhancement factor around 0.90 to 2.70 depending on *TR*, *Re* and twisted rotational. The numerical results reveal that the maximum *TEF* is found to be about 2.7 at *Re* = 2000, *TR* = 2 for co–rotating case.

4.6 Comparison with single twisted tape

The comparisons between single twisted tape and double twisted tapes can be divided into three parts; heat transfer, friction factor and thermal enhancement factor as depicted in Figs. 14a, b and c, respectively. The single twisted tape performs higher heat transfer rate than the double twisted tapes when the Reynolds number higher than 1000 for all *TR* values. At *TR* = 2, Nu/Nu_0 is found around 8.2, 7.3 and 6 for single twisted tape, co–rotating double twisted tapes and counter–rotating double twisted tapes, respectively.

The double twisted tapes give higher friction factor than the single twisted tape for all *TR* and *Re* values. The f/f_0 is found to be around 16, 18.5 and 18.5, respectively, for single twisted tape, co–rotating double twisted tapes and counter–rotating double twisted tape at *TR* = 2 and *Re* = 2000.

As Fig. 14c, it is found that the maximum thermal enhancement factor is found at *TR* = 4 and 2 for the single twisted tape and the co–rotating twisted tapes, respectively, while the thermal enhancement factor for counter–rotating case shows nearly values for all *TR* values. At *TR* = 2, the single twisted tape gives higher *TEF* than the co–rotating double twisted tapes when the Reynolds number higher than 800.

The correlations for Nu/Nu_0 and f/f_0 in the studies range are developed. The resultant correlations reveal that Nu/Nu_0 is affected by Reynolds number (*Re*), Prandtl number (*Pr*) and twisted ratio (*TR*) while the f/f_0 are depended on Reynolds number (*Re*) and twisted ratio (*TR*). The correlations of the Nu/Nu_0 for co–rotating and counter–rotating cases are presented as Eqs. 12 and 13, respectively, while the correlations of f/f_0 are shown in Eqs. 14 and 15, respectively. Evidently, the predicted Nu/Nu_0 and f/f_0 are within ±10% of the numerical data for both cases as depicted in Figs. 15 and 16, respectively.

$$Nu/Nu_0 = 0.362\,\mathrm{Re}^{0.423} PR^{0.4} TR^{-0.263}, \text{ co–rotating case} \tag{12}$$

$$Nu/Nu_0 = 0.471\,\mathrm{Re}^{0.372} PR^{0.4} TR^{-0.222}, \text{ counter–rotating case} \tag{13}$$

$$f/f_0 = 0.896\,\mathrm{Re}^{0.403} TR^{-0.371}, \text{ co–rotating case} \tag{14}$$

$$f/f_0 = 0.913\,\mathrm{Re}^{0.399} TR^{-0.362}, \text{ counter–rotating case} \tag{15}$$

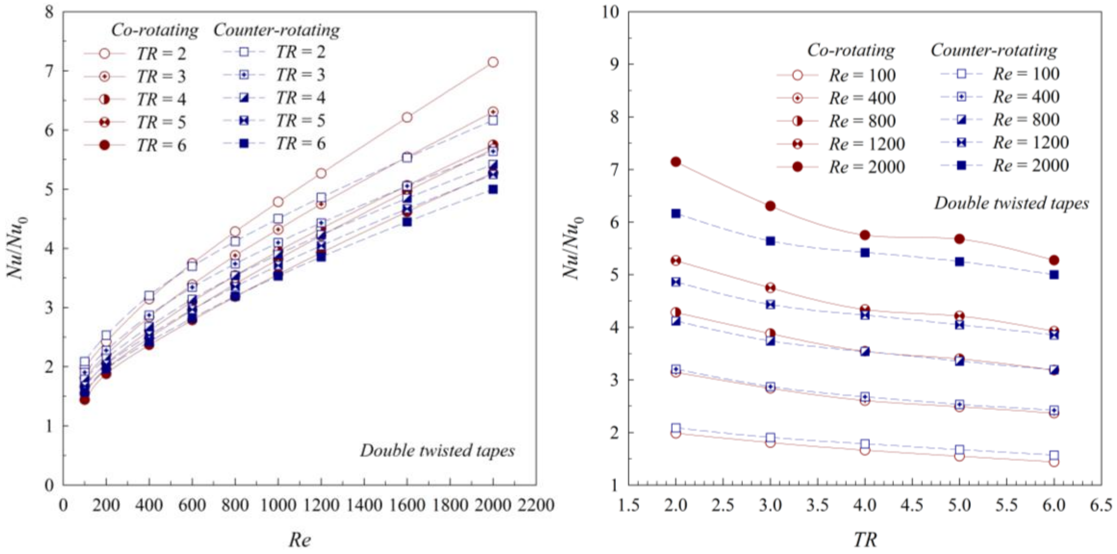

(a) (b)

Figure 11: (a) Variations of Nu/Nu_0 with Reynolds number and (b) Variations of Nu/Nu_0 with *TR* for double twisted tapes.

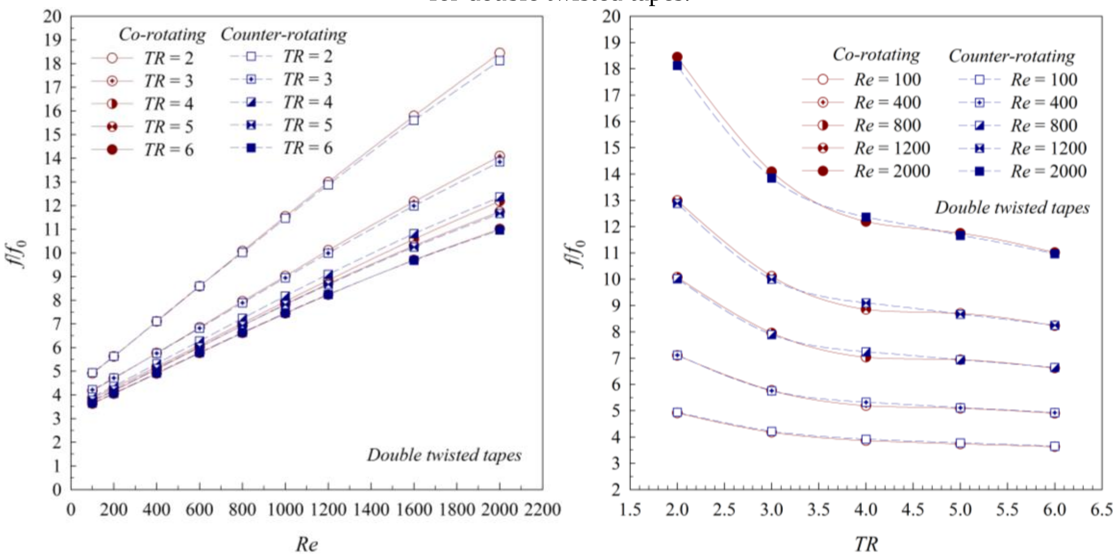

(a) (b)

Figure: 12 (a) Variations of f/f_0 with Reynolds number and (b) Variations of f/f_0 with *TR* for double twisted tapes.

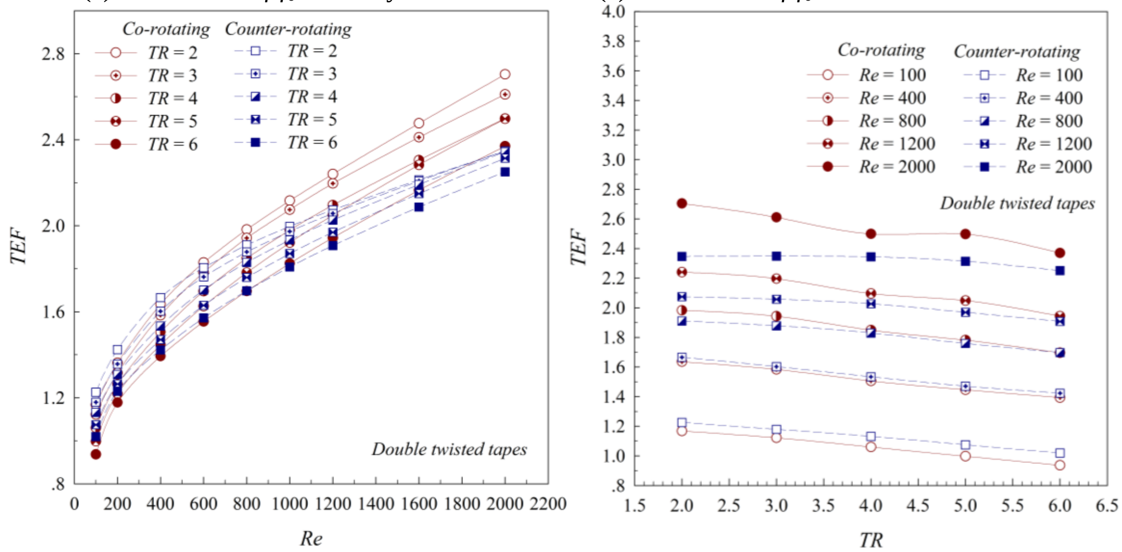

(a) (b)

Figure 13: (a) Variations of *TEF* with Reynolds number and (b) Variations of *TEF* with *TR* for double twisted tapes.

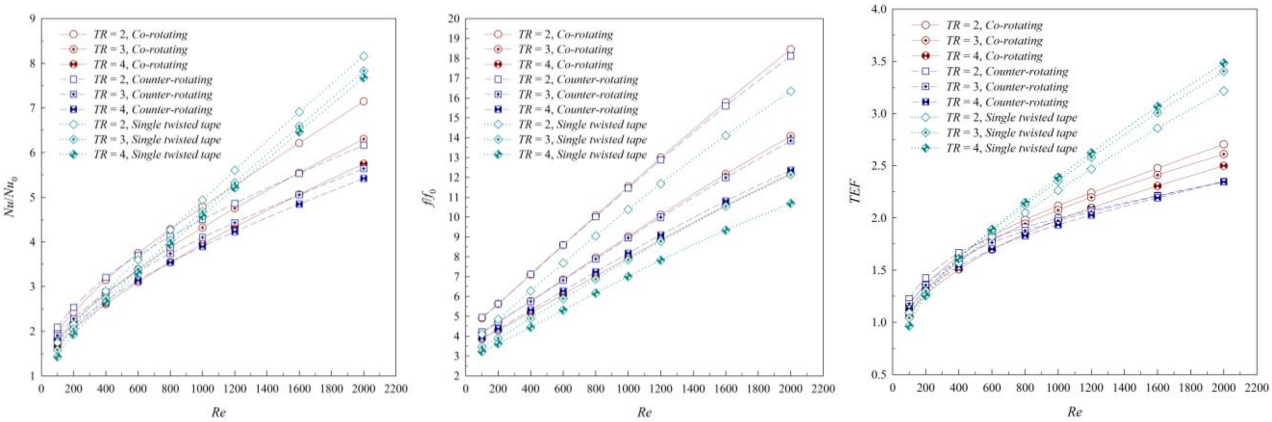

(a) (b) (c)

Figure 14: Comparisons between single twisted tape and double twisted tapes for (a) Nu/Nu_0, (b) f/f_0 and (c) *TEF*.

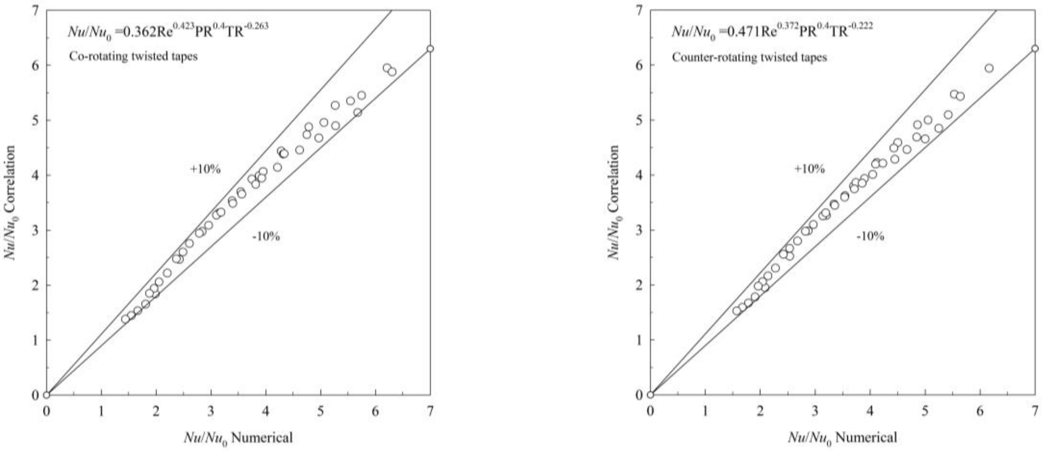

(a) (b)

Figure 15: Correlations of Nu/Nu_0 for (a) co–rotating case and (b) counter–rotating case double twisted tapes.

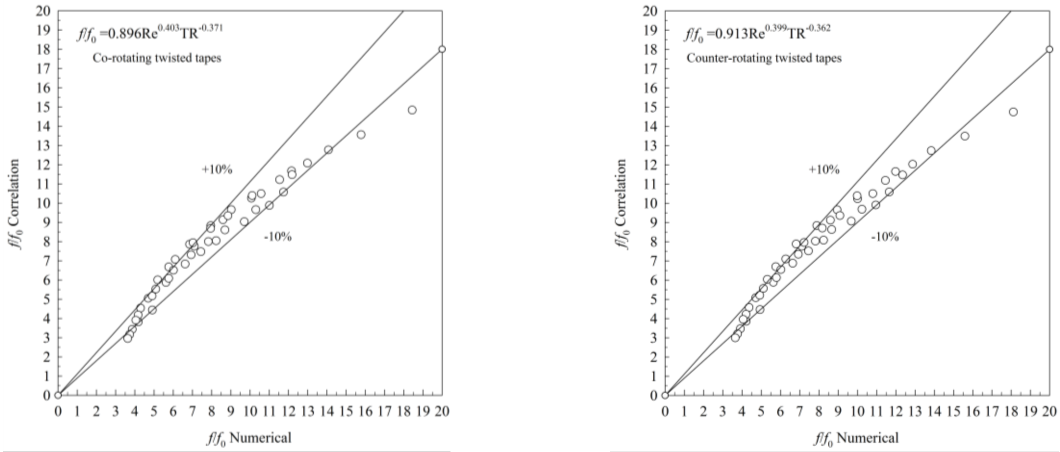

(a) (b)

Figure 16: Correlations of f/f_0 for (a) co–rotating case and (b) counter–rotating case double twisted tapes.

5. CONCLUSIONS

In this paper, laminar fully developed periodic flow configurations and heat transfer characteristics in the circular tube with co–rotating and counter–rotating double twisted tapes have been investigated numerically. The major findings are summarized as follows:

- The four and two main vortex flows which created by using co–rotating and counter–rotating double twisted tapes, respectively, can help to enhance heat transfer rate in the test tube when compared with smooth tube.
- The decrease in twisted ratio results in the increase in heat transfer rate and friction factor for all Reynolds

numbers.

- The co–rotating case gives higher heat transfer than the counter–rotating case at all *TR* values. The friction factor ratios for both cases provide nearly values for all *TR* and Reynolds number values.
- In range examined, the order of heat transfer enhancement is about 1.4 to 7.3, for using the double twisted tape with *TR* = 1.00 – 6.00. However, the heat transfer augmentation is associated with enlarged pressure loss ranging from 3.50 to 18.50 times above the smooth circular tube.
- Thermal enhancement factors for the double twisted tape are found to be in a range of 0.90 – 2.70 indicating higher thermal performance over the smooth tube, depending on *TR*, Re and twisted tape rotational.
- The single twisted tape performs higher heat transfer rate and thermal enhancement factor than double twisted tapes when the Reynolds number higher than 800 at a similar twisted ratio.

NOMENCLATURE

D	hydraulic diameter of tube, m
f	friction factor
h	convective heat transfer coefficient, W m^{-2} K^{-1}
k	thermal conductivity, W m^{-1} K^{-1}
Nu	Nusselt number ($=hD/k$)
p	static pressure, Pa
Pr	Prandtl number (Pr = 0.707)
Re	Reynolds number ($=\rho UD/\mu$)
T	temperature, K
TR	twisted ratio (y/W)
U	mean velocity in channel, m s^{-1}
W	width of twisted tape
y	twisted pitch
Greek letter	
μ	dynamic viscosity, kg $s^{-1}m^{-1}$
Γ	thermal diffusivity
TEF	thermal enhancement factor, $(=(Nu/Nu_0)/(f/f_0)^{1/3})$
ρ	density, kg m^{-3}
Subscript	
0	smooth channel
in	inlet
pp	pumping power
w	wall

6. ACKNOWLEDGEMENT

The author would like to thank the King Mongkut's University of Technology North Bangkok (KMUTNB) research fund, Dr. Withada Jedsadaratanachai, Assoc. Prof. Dr. Pongjet Promvonge and Mr. Pitak Promthaisong for suggestions.

7. REFERENCES

[1] S. Eiamsa-ard, C. Thianpong, P. Eiamsa-ard, P. Promvonge, "Convective heat transfer in a circular tube with short-length twisted tape insert", International Communication in Heat and Mass Transfer, Elsevier, vol. 36, no. 4, pp. 365–371, 2009.

[2] S. Eiamsa-ard, C. Thianpong, P. Promvonge, "Experimental investigation of heat transfer and flow friction in a circular tube fitted with regularly spaced twisted tape elements", International Communication in Heat and Mass Transfer, Elsevier, vol. 33, no. 10, pp. 1225–1233, 2006.

[3] P.K. Pal, S.K. Saha, "Experimental investigation of laminar flow of viscous oil through a circular tube having integral spiral corrugation roughness and fitted with twisted tapes with oblique teeth", Experimental Thermal and Fluid Science, Elsevier, vol. 57, pp. 301–309, 2014.

[4] S. Pal, S.K. Saha, "Laminar flow and heat transfer through a circular tube having integral transverse corrugations and fitted with centre-cleared twisted-tape", Experimental Thermal and Fluid Science, Elsevier, vol. 57, pp. 388–395, 2014.

[5] S.W. Chang, M.H. Guo, "Thermal performances of enhanced smooth and spiky twisted tapes for laminar and turbulent tubular flows", International Journal of Heat and Mass Transfer, Elsevier, vol. 55, Issues 25–26, pp. 7651–7667, 2012.

[6] P. Promvonge, S. Pethkool, M. Pimsarn, C. Thianpong, "Heat transfer augmentation in a helical-ribbed tube with double twisted tape inserts", International Communications in Heat and Mass Transfer, Elsevier, vol. 39, Issue 7, pp. 953–959, 2012.

[7] H. Bas, V. Ozceyhan, "Heat transfer enhancement in a tube with twisted tape inserts placed separately from the tube wall", Experimental Thermal and Fluid Science, Elsevier, vol. 41, pp. 51–58, 2012.

[8] M.M.K. Bhuiya, A.S.M. Sayem, M. Islam, M.S.U. Chowdhury, M. Shahabuddin, "Performance assessment in a heat exchanger tube fitted with double counter twisted tape inserts", International Communications in Heat and Mass Transfer, Elsevier, vol. 50, pp. 25–33, 2014.

[9] S. Eiamsa-ard, K. Yongsiri, K. Nanan, C. Thianpong, "Heat transfer augmentation by helically twisted tapes as swirl and turbulence promoters", Chemical Engineering and Processing: Process Intensification, Elsevier, vol. 60, pp. 42–48, 2012.

[10] M.M.K. Bhuiya, M.S.U. Chowdhury, M. Shahabuddin, M. Saha, L.A. Memon, "Thermal characteristics in a heat exchanger tube fitted with triple twisted tape inserts", International Communications in Heat and Mass Transfer, Elsevier, vol. 48, pp. 124–132, 2013.

[11] M.M.K. Bhuiya, M.S.U. Chowdhury, M. Saha, M.T. Islam, "Heat transfer and friction factor characteristics in turbulent flow through a tube fitted with perforated twisted tape inserts", International Communications in Heat and Mass Transfer, Elsevier, vol. 46, pp. 49–57, 2013.

[12] S.W. Chang, T.L. Yang, J.S. Liou, "Heat transfer and pressure drop in tube with broken twisted tape insert", Experimental Thermal and Fluid Science, Elsevier, vol. 32, no. 2, pp. 489–501, 2007.

[13] P. Seemawute, S. Eiamsa-ard, "Thermohydraulics of turbulent flow through a round tube by a peripherally-cut twisted tape with an alternate axis", International Communications in Heat and Mass Transfer, Elsevier, vol. 37, pp. 652–659, 2010.

[14] S. Bhattacharyya, S.K. Saha, "Thermohydraulics of laminar flow through a circular tube having integral helical rib roughness and fitted with centre–cleared twisted–tape", Experimental Thermal and Fluid Science, Elsevier, vol. 42, pp. 154–162, 2012.

[15] C. Thianpong, P. Eiamsa-ard, P. Promvonge, S. Eiamsa-ard, "Effect of perforated twisted-tapes with parallel wings on heat tansfer enhancement in a heat exchanger tube", Energy Procedia, Elsevier, vol. 14, pp. 1117–1123, 2012.

[16] P. Promvonge, S. Eiamsa-ard, "Heat transfer behaviors in a tube with combined conical-ring and twisted-tape insert", International Communications in Heat and Mass Transfer, Elsevier, vol. 34, pp. 849–859, 2007.

[17] S. Eiamsa-ard, K. Wongcharee, S. Sripattanapipat, "3-D numerical simulation of swirling flow and convective heat transfer in a circular tube induced by means of loose-fit twisted tapes", International Communications in Heat and Mass Transfer, Elsevier, vol. 36, pp. 947–955, 2009.

[18] P. Eiamsa-ard, N. Piriyarungroj, C. Thianpong, S. Eiamsa-ard, "A case study on thermal performance assessment of a heat exchanger tube equipped with regularly-spaced twisted tapes as swirl generators", Case Studies in Thermal Engineering, Elsevier, vol. 3, pp. 86–102, 2014.

[19] X. Zhang, Z. Liu, W. Liu, "Numerical studies on heat transfer and flow characteristics for laminar flow in a tube with multiple regularly spaced twisted tapes", International Journal of Thermal Sciences, Elsevier, vol. 58, pp. 157–167, 2012.

[20] J. Guo, A. Fan, X. Zhang, W. Liu, "A numerical study on heat transfer and friction factor characteristics of laminar flow in a circular tube fitted with center cleared twisted tape", International Journal of Thermal Science, Elsevier, vol. 50, pp. 1263–1270, 2011.

[21] S. Eiamsa-ard, P. Seemawute, "Decaying swirl flow in round tubes with short-length twisted tapes", International Communications in Heat and Mass Transfer, Elsevier, vol. 39, Issue 5, pp. 649–656, 2012.

[22] Y. Hong, X. Deng, L. Zhang, "3D Numerical Study on Compound Heat Transfer Enhancement of Converging-diverging Tubes Equipped with Twin Twisted Tapes", Chinese Journal of Chemical Engineering, Elsevier, vol. 20, Issue 3, pp. 589–601, 2012.

[23] P. Promvonge, S. Sripattanapipat, S. Kwankaomeng, "Laminar periodic flow and heat transfer in square channel with 45^o inline baffles on two opposite walls", International Journal of Thermal Science, Elsevier, vol. 49, pp. 963–975, 2010.

[24] W. Jedsadaratanachai, S. Suwannapan and P. Promvonge, "Numerical study of laminar heat transfer in baffled square channel with various pitches", Energy Procedia, Elsevier, vol. 9, pp. 630 – 642, 2011.

[25] S. Kwankaomeng, P. Promvonge, "Numerical prediction on laminar heat transfer in square duct with 30° angled baffle on one wall", International Journal of Heat and Mass Transfer, Elsevier, vol. 37, pp. 857–866, 2010.

[26] P. Promvonge, W. Jedsadaratanachai, S. Kwankaomeng, "Numerical study of laminar flow and heat transfer in square channel with 30 inline angled baffle turbulators", Applied Thermal Engineering, Elsevier, vol. 30, pp. 1292–1303, 2010.

[27] W. Jedsadaratanachai and A. Boonloi, "Effect of twisted ratio on flow structure, heat transfer and thermal improvement in a circular tube with single twisted tape", Journal of Mathematics and Statistics, Science publications, vol. 10, pp. 80–91, 2014.

[28] S.V. Patankar, Numerical heat transfer and fluid flow, McGraw-Hill, New York, 1980.

[29] F. Incropera, P.D. Dewitt, Introduction to Heat Transfer, 5rd ed., John Wiley & Sons, 2006.